Published in final edited form as:
Langmuir. 2012 November 27; 28(47): 16318–16326. doi:10.1021/la302654s.

The Role of Nanoparticle Surface Functionality in the Disruption of Model Cell Membranes

Babak Y. Moghadam[†], **Wen-Che Hou**[‡], **Charlie Corredor**[†], **Paul Westerhoff**[‡], and **Jonathan D. Posner**[*,†]

[†]Mechanical Engineering, Chemical Engineering, University of Washington, Seattle, WA 98195

[‡]School of Sustainable Engineering and the Built Environment, Arizona State University, Tempe, Arizona 85287-5306

Abstract

Lipid bilayers are biomembranes common to cellular life and constitute a continuous barrier between cells and their environment. Understanding the interaction of engineered nanomaterials (ENMs) with lipid bilayers is an important step toward predicting subsequent biological effects. In this study, we assess the effect of varying the surface functionality and concentration of 10 nm-diameter gold (Au) and titanium dioxide (TiO2) ENMs on the disruption of negatively charged lipid bilayer vesicles (liposomes) using a dye leakage assay. Our findings show that Au ENMs having both positive and negative surface charge induce leakage that reaches a steady state after several hours. Positively charged particles with identical surface functionality and different core composition show similar leakage effects and result in faster and greater leakage than negatively charged particles, which suggests that surface functionality, not particle core composition, is a critical factor in determining the interaction between ENMs and lipid bilayers. The results suggest that particles permanently adsorb to bilayers and that only one positively charged particle is required to disrupt a liposome and trigger leakage of its entire contents in contrast to mellitin molecules, the most widely studied membrane lytic peptide, which requires hundred of molecules to generate leakage.

Keywords

Nanomaterials; Lipid bilayer; Toxicity; Nanotechnology

1. INTRODUCTION

Engineered nanomaterials (ENMs) are used in more than 1300 commercial products. Whether by design or as unintended consequence, ENMs may contact human, bacteria or other cells which has led to the growing public debates on if potential impacts of these materials on the environment and human health outweigh their benefits.[1,2] ENMs have several potential exposure routes such as incidental or intended inhalation, ingestion, skin uptake, and injection. Recent toxicological studies have suggested that ENMs may cause adverse health effects based on their chemical composition, shape and size, but the fundamental cause effect relationships are not well understood and thus, the interaction of nanomaterials with biological systems including living cells requires additional research.[3–13]

[*]Corresponding Author: jposner@uw.edu (J.D.P). Tel: +1 (206) 543-9834. Fax: +1 (206) 685-8047.

Supporting Information

Additional information on liposomes number density calculations, and Carboxyfluorescein calibration curves. This material is available free of charge via the Internet at http://pubs.acs.org.

The phospholipid bilayers in liquid-crystalline phase (as oppose to gel phase) are a fundamental structural element of the cell membrane and common to cellular life.[14] The lipid bilayer of a cell membrane serves as continuous barrier between cellular content and its local environment as well as serves as the interface where chemical fluxes are regulated by various membrane-bound proteins. Therefore, synthesized lipid bilayers are a critical model interface to study nano-bio interactions.[15] Model lipid bilayers have previously been shown to exhibit mechanical and electrical properties similar to those of cell membranes[16] and thus offer significant potential for systematically probing the role of specific membrane properties (lipid composition, charge, fluidity, etc.) on cell membrane interactions with ENM. A range of experimental techniques have shown that the ENMs interaction with lipid bilayers depends on their physicochemical properties.[17–19]

Various lipid bilayer structures, i.e. supported, suspended and vesicles, along with different detection techniques have been used to probe the effects of ENMs on lipid bilayer. Hong et al. and Mecke et al. investigated the interaction of poly (amidoamine) dendrimers with solid supported 1,2-dimyristoyl-sn-glycero-3-phosphocholine (DMPC) lipid bilayers using atomic force microscopy (AFM). [20,21] They showed that positively charged dendrimers create holes on supported lipid bilayers, dendrimers with lower surface charge don't initiate holes but expanded existing defects, and neutrally charged dendrimers did not cause hole formation at the same concentration range. Leroueil et al., also used AFM to show that disruption of solid supported lipid bilayers (SSLB) is a common property of cationic nanomaterials regardless of shape, chemical composition, deformability, charge, or size.[22]

Our recent work shows that ENMs significantly adsorb to bilayers. We quantified the distribution of fullerene [23] and gold [24] ENMs between (SSLB) and water. This work indicates that water-lipid distribution reaches some steady state distribution on lipid bilayer. The adsorption increases with decreasing pH, suggesting that electrostatic interactions are important. These studies suggest that the distribution of ENM between lipid bilayers and water also have the potential to predict bioaccumulation of ENMs in organisms, analogous to how octanol-water partitioning is used for molecular compounds.[25]

Being supported on a solid surface limits SSLB's capability in detecting the leakage and ENMs transfer through bilayers. Several groups, including our own, have probed change in ionic permeability of suspended lipid bilayers using electrophysiological measurements.[26–29] The complexity of the experimental setup, e.g. high sensitivity to vibrations, and having low signal to noise ratios at high ionic strength mediums, limit their application to be used in high-throughput assays.

Lipid bilayer vesicles (liposomes) are synthetic mimics of cellular membranes and represent an experimental system widely used for more than 30 years in the field of biochemical research involving lipids. Vesicles with different structures are used extensively in drug delivery and combinatory chemotherapeutic systems and can also be used to study artificial cell formation, which primitively mimics the membrane-based structure of eukaryotic cells.[30] Hybrid lipid vesicle-nanoparticles have been shown to stabilize nanoparticles in bio-medical applications.[31] Liposomes maintain natural fluidity of lipid bilayers, in contrast to supported lipid bilayer where binding of the inner layer of lipid to the solid surface may decrease fluidity of the lipid bilayer.[32] The defined size, composition, homogeneity, and availability of large-batch production of liposomes have made them useful for the study of diverse cellular phenomena.[33] In many cases, however, the successful use of liposomes depends on their formulation and the method of preparation and can be used for robust high-throughput screening assays.[34]

Liposome leakage assays have been used extensively to probe the lipid bilayer response to macromolecules such as melittin peptides and other bio molecules, like magainin, cecropin and alamethicin.[35–37, 38] The assay is based on measuring the increase fluorescence that results from the leakage of self-quenched dye that is loaded into liposomes. The self-quenching property of fluorescence dye permits leakage from liposomes to be monitored continuously and is sensitive to small perturbations in the bilayer.[39] This method can also be used to gain some mechanistic understanding by which ENM induce liposome leakage, e.g. by monitoring dye self-quenching efficiency to determine mode of interaction, etc.[40–42]

Some recent studies use liposome leakage assays to determine the effect of ENMs on lipid bilayers. Hirano et al. studied the influence of single walled carbon nanotubes (SWNTs) conjugated with positively charged lysozymes (LSZ) on the leakage of negatively charged 200 nm unilamellar 1,2-dioleoyl-sn-glycero-3-phosphogrycrol (DOPG)/1,2-dioleoyl-sn-glycero-3-phosphocholine (DOPC) liposomes. [43] They reported significant leakage caused by SWNTs-LSZ conjugates, while only marginal leakage occurred by bare SWNTs and unbounded LSZ, concluding that both SWNTs and LSZ have no effect on liposomes unless they are conjugated together, i.e. surface functionality is important. The effect of ENMs on liposomes correlates well with in vitro cell studies. Goodman et al. compared the cellular toxicity of 2 nm gold ENMs with liposome leakage assays. [44] They showed that cationic materials are moderately toxic and that anionic materials are nontoxic which correlated well with their lytic effects on L-α-stearoyl-oleoyl-phosphotidylcholine (SOPC) and L-α-stearoyl-oleoyl-phosphotidylserine (SOPS) lipid bilayer vesicle-disruption assays. These previous studies use liposomes larger than 200 nm in diameter, made by extrusion technique, which are most likely to be multilamellar vesicles (MLV). The size, heterogeneity and the presence of many internal compartments make MLVs more resistant to defects and disruption than unilamellar vesicles and limit their use in studies of bilayer properties such as permeability and fusion.[45,46,47] Large unilamellar vesicles (LUVs) are relatively homogeneous in size, contain relatively large volumes (results in higher assay SNRs) and more closely resemble the structure of cell membranes.[48]

In this work, we investigate the role of surface functionality and charge of 10 nm gold (Au) and titanium dioxide (TiO2) ENMs on the disruption of DOPC LUVs (~100 nm) using a liposome dye leakage assay. The use of LUVs assures that the ENMs are interacting with a single layer of lipid bilayer. We present leakage kinetics as a function of particle surface functionality and concentration. We develop a kinetic model to describe the rate and time constant of interaction and show that the rate constant is a property of each ENM with specific surface functionality. The ENM-induced disruption is compared with melittin, a toxic peptide consisting of 26 amino acids that is well-known to create pores on lipid membranes.[35,40,49] Mass concentration, number density, as well as ENM number and mass to lipid ratio descriptions are used to shed light on the possible interaction mechanism of liposomes disruption.

2. EXPERIMENTAL SECTION

2.1. Materials

We use DOPC dissolved in chloroform (CAS# 4235-95-4, Avanti Polar Lipids, Alabaster, AL). We dissolved melittin (96% pure, CAS# 20449-79-0, Sigma Aldrich chemicals, Saint Louis, MO) in 20 mM HEPES (CAS# 7365-45-9, Sigma Aldrich chemicals, Saint Louis, MO) buffer at pH = 7.4. The resulting stock melittin solution (5 mg/mL) was then frozen and kept at −20°C until used. Triton X-100 (CAS# 90002-93-1, Fisher Scientific, Hampton, NH) and 5(6)-carboxyfluoresceine (CF) (CAS# 72088-94-9, Molecular Probes, Eugene, OR) are used without further purification. To facilitate CF crystals dissolution in water, the aqueous stock solution of 100 mM CF was prepared in 20 mM HEPES, adjusting to pH =

7.4 with KOH solution (10 M). Commercially available ENMs were used, all with reported diameters of 10 nm. We use Au and TiO_2 ENMs functionalized with polydiallyldimethylammonium chloride (polyDADMAC) (Vive Nano, Toronto, ON), Au coated with tannic acid and polyvinylpyrrolidone (PVP) (NanoComposix, San Diego, CA), and TiO_2 functionalized with sodium polyacrylate. All the ENMs were chosen with the same nominal size (*i.e.* 10 nm), to be relatively small compared to the liposomes, as well as commercially available with a variety of surface functionality and charge. Note that TiO_2 particles have the highest known production volume and use in commercial product.[50] Gold particles have become a standard for academic research because they are available in a wide range of sizes and surface functionalities and are easy to image using electron microscopy and detect in low concentrations in complex matrices. Poly DADMAC (CAS# 26062-79-3, Sigma Aldrich chemicals, Saint Louis, MO) was obtained as an isolated compound to observe its disruption effect independent from the nanoparticles. All aqueous samples were prepared using water purified with a Milli-Q Advantage A10 ® system (Millipore Corp., Billerica, MA).

2.2. Liposome preparation

We prepared liposomes using the extrusion method.[51,52] First, a 25 mg/mL solution of DOPC in chloroform was dried under a gentle stream of pure nitrogen, to create thin layers of dried lipid. The residual solvent was removed in vacuum overnight in a desiccator at room temperature. After drying, we hydrate the lipid films in HEPES buffer (pH 7.4, 20 mM) containing 100 mM CF. We kept the buffer concentration at an optimized value (*i.e.* 20 mM) in order to prevent ENM's aggregation while performing leakage experiments. The lipid mixture was incubated for 1 h with occasional vortex mixing at 20°C, above the phase transition temperature of the phospholipid component of DOPC liposomes (−19°C). We then subject the lipid mixture to five freeze-thaw cycles in liquid nitrogen and then extrude (Northern Lipids, Vancouver, BC) them 20 times through a stack of two polycarbonate membrane filters of 100 nm pore size (model# 110605, Whatman, Clifton, NJ). We remove CF that is not trapped in the liposomes using a 3kDa centrifugal ultrafiltration filters (model# UFC900308, Millipore Corp., Billerica, MA) and resuspend in HEPES buffer without CF dye. The resulting 100 nm liposome stock suspension has a final lipid concentration of 2.54 mM, as measured using the malachite green dye method.[53] We measure the liposome size distribution using dynamic light scattering before and after the removal of encapsulate dye. Our t-test calculations shows that there is not a statistically significant difference (at significance level of $\alpha = 0.05$) between the mean diameter of the two liposome samples. We measured the final mean diameter of liposomes as 106.2 ± 3.3 nm (95% confidence interval). The prepared liposome suspensions were stored at 4°C and used within 2 weeks of preparation.

2.3. Leakage experiment

We performed dye leakage experiments by mixing CF dye encapsulated liposomes and ENMs. All the samples were kept in amber vials and covered with aluminum foil to reduce effect of light on chemical and physical properties of reagents. The stock liposome dispersion was diluted with 20 mM HEPES buffer in order to obtain a phospholipid concentration of 7.8 μM in a 3.5 ml methacrylate fluorometer cuvettes (Perfector Scientific, Atascadero, CA). The initial vesicle dispersion has a low background fluorescence intensity, we denote as I_0, because the high concentration (>50 mM) of CF dye encapsulated in the liposomes is self-quenching. The CF calibration curve in 20 mM HEPES buffer at pH=7.4 is provided in the supporting information. An aliquot of ENM solution was added to the liposome dispersion to obtain desired ENM to lipid ratio. The ENMs induce the release of CF from the liposomes which results in dilution of the dye into the electrolyte and a

measured increase in fluorescence. We report the time dependent leakage as the normalized fraction of released CF given by,

$$L(t)=\frac{I(t)-I_0}{I_{max}-I_0} \quad (1)$$

Where $I(t)$ is the time dependent fluorescence intensity, I_0 is the initial intensity before addition of ENMs, and I_{max} is the maximum fluorescent intensity upon the complete leakage of dye, which is induced by addition of Triton X-100 at final concentration of 32 mM to each experimental sample after the fluorescence intensity reached a steady value. Triplicate samples were prepared for several ENM to lipid ratios to ensure the reproducibility of the experiments.

2.4. Analysis

The hydrodynamic sizes and zeta potentials of ENMs and liposomes were determined using dynamic light scattering (DLS) (NICOMP 380 ZLS, Particle Sizing Systems, Santa Barbara, CA) that uses a laser light at 635 nm. The measurements were done under a scattering angle of 90° at 20°C. All ENM sizes are reported as intensity-weighted sizes. For the leakage experiments we used a spectrofluorometer (LS-5, Perkin-Elmer, Waltham, MA) with excitation wavelength of 490 nm and emission at 517 nm (excitation and emission slit widths were 2.5 nm).

2.5. Transmission electron microscopy studies

The transmission microscopy investigations were performed with a CM12 transmission electron microscope (TEM) (Philips, Amsterdam, Netherlands). All the images were recorded at accelerating voltage of 80kV using a CCD camera (Gatan, Pleasanton, CA) with a chip that was cooled to −30°C.

Briefly, the method for sample preparation was as follows, with a more comprehensive description available in Thery *et al.*[54] 7 μL of liposomes solution in 20 mM HEPES was mixed with 1 μL of 8% paraformaldehyde and incubated for 5 minutes. Then, we applied a drop of sample to parafilm and floated the grid on top of the drop for 20 min at STP condition. Next, we washed twice for 5 min with buffer and incubated on 1% aqueous glutaraldehyde for 5 min. The sample is then washed one more time with deionized water, incubated on uranyl oxalate at pH 7 for 5 min, and incubated on 1.8% methyl cellulose 0.4% uranyl acetate for 10 min in the presence of ice. Finally, the grid was covered with petri dish and allowed to air-dry.

3. Results and discussion

3.1. Liposome and ENMs Characterization

We measured the hydrodynamic diameter and zeta potentials of the ENMs and DOPC liposomes in the same HEPES buffer that the interaction experiments of liposomes and ENMs were conducted (*i.e.*, in 20 mM HEPES buffer electrolyte at pH = 7.4). We measured the hydrodynamic size and zeta potential of DOPC liposomes as 106.2 ± 4.4 nm and −12.1 ± 1.1 mV, respectively. The hydrodynamic size of DADMAC coated gold (Au DAD), tannic acid coated gold (Au TAN) and PVP coated gold (Au PVP) were measured as 16.2 ± 1.6 nm, 18.2 ± 3.9 nm and 21.9 ± 5.5 nm, respectively. These measured sizes are marginally larger than size revealed by TEM images (reported by the manufacturer), potentially due to the incorporation of surface coating or slight aggregation in the DLS measurements. Au DADs have a zeta potential of 22 ± 2.4 mV, while Au TAN and Au PVP were both −36.8 ±

1.3 mV. DLS measurements indicate the hydrodynamic sizes of DADMAC coated titanium dioxide (TiO_2 DAD) and sodium polyacrylate coated titanium dioxide (TiO_2 SOD) were 10.9 ± 0.2 nm and 7.7 ± 0.3 nm, respectively. The zeta potentials for TiO_2 DAD and TiO_2 SOD were 31.2 ± 1.0 mV and −45.8 ± 0.4 mV, respectively at pH = 7.4.

3.2. Kinetics of liposome leakage

Au ENMs induce liposome leakage in a time-dependent manner. Figure 1A shows the time dependent dye leakage, *L(t)*, for Au DAD, Au TAN, Au PVP, melittin, and a control sample with liposomes present only.

We normalize particle concentration (mg/L) with the lipid concentration (mg/L) and report it as the mass concentration ratio m_P/m_{LP} (mg/mg) in order to compare our leakage data to other experimental data where different lipid concentrations have been used. Au DADs induce rapid leakage that increases exponentially and reaches a steady state value after a few hours. At concentration ratios larger than 0.015 (mg/mg), complete release of dye is observed after 6 hours. At m_P/m_{LP} of 0.002 (mg/mg), the leakage was indistinguishable from the control experiment, in which ENMs were absent. In the control experiment, leakage still occurred at a much slower rate, which we attribute to the natural decay of liposomes. This suggests that Au DAD requires $m_P/m_{LP} > 0.002$ (mg/mg) to mediate significant liposome leakage. The leakage induced by Au DADs at $m_P/m_{LP} = 0.005$ (mg/mg) reaches 40% at steady state, suggesting that Au DADs remain on the bilayer surface not attaching to other liposomes, otherwise we should have observed continued increase in the leakage until all the dye has been released from all the liposomes. In a related study by Goodman *et al.*, they reported that 2 nm positively charged Au ENMs at 43 ppb induce a 20% steady state leakage from 1 μm negatively charged SOPC/SOPS vesicles after 5 min, while our results show a 40% steady state leakage induced by 10 nm Au DADs (30 ppb) after 90 min. The faster kinetics in their system to reach a steady state leakage can be attributed to the smaller ENM size they used (*i.e.*, 2 nm) resulting in higher diffusivity for positively charged Au ENMs compared to our 16 nm Au DADs, while the lower level of steady state leakage they recorded might be due to lower number density ratio of their assay compare to ours.

The Au TAN and Au PVP exhibit weak leakage compare to the control sample even at high concentration ratios (*i.e.* 0.02). Close inspection of the data suggests that the negatively charged ENMs stabilize the liposomes to some degree (verified using t-test). We believe that this slow leakage is a result of electrostatic repulsion of the negatively charged ENMs and vesicles. Close inspection of the data suggests that the negatively charged ENMs stabilize the liposomes to some degree. Zhang et al showed that adding negatively charged 20 nm polystyrene (PS) latex ENMs stabilize 200 nm DLPC liposomes resulting in reduction of the leakage caused by fusion of liposomes with one another.[55]

We compare the ENMs-induced leakage to melittin, a well-known bilayer disruptor. Melittin induces complete leakage rapidly (<30 min) at mass ratios greater than 0.005 (mg/mg). One reason for the fast kinetics of melittin is its high number density compare to Au ENMs for an equivalent mass ratio. Melittin has an order of magnitude larger diffusivity (1.92×10^{-6} cm^2/s) than Au ENMs (2.06×10^{-7} cm^2/s), based on the Stokes-Einstein equation and our DLS measured hydrodynamic size of melittin as 2.5 ± 1.0 nm in 20 mM HEPES at pH=7.4.

Lacowicz *et. al*[56] also measured site-to-site (distance between sites on labeled macromolecules) diffusion coefficient of melittin in water as 3.38×10^{-7} cm^2/s using fluorescence energy resonance transfer (FRET). Our melittin kinetic data follows the same increasing trend as an earlier study by Wessman *et al.*, where liposomes with the same size and lipid composition have been used. [57] According to their measurements, at melittin to

lipid concentration ratio of m_P/m_{LP}=0.025 (mg/mg) (5 fold smaller than one we have used) complete leakage occurs after 7 minutes.

3.3. Modeling leakage kinetic

We determined characteristic leakage rate constants by modeling our kinetic data presented in Fig. 1 using Lagergren's pseudo-first order adsorption model.[58,59,60] The rate of leakage is proportional to the initial ENM to lipid mass ratio m_P/m_{LP} in the extravesicullar medium (considered as a reservoir) and the fraction of undisturbed liposomes ($1-L(t)/L_\infty$), where L_∞ is the steady state leakage for a given particle and mass concentration ratio. The leakage rate per unit time is,

$$\frac{dL}{dt}=K_L\frac{m_P}{m_{LP}}\left(1-\frac{L(t)}{L_\infty}\right) \quad (2)$$

where the leakage rate constant is K_L (in S^{-1}). Integrating with the initial condition at $t = 0$ of $L(t) = 0$ the time dependent leakage induced by ENMs is,

$$L(t)=L_\infty\left(1-\exp\left(-K_L\frac{m_P}{m_{LP}}\frac{1}{L_\infty}t\right)\right) \quad (3)$$

Equation 3 is shown fit to the data in Figure 1 where the mass ratios (m_P/m_{LP}) and L_∞ are measured quantities and the rate constant K_L is a fitting parameter that remains constant for a specific surface functionality. The leakage reaches a steady value with a characteristic time constant of $\tau = (L_{eq}/K_L)\,(m_P/m_{LP})$. The rate and time constants and are presented in Table 1 along with 95% confidence intervals (based on Student's t statistics). The model fits the concentration and time dependent trends. The values of τ decreases with concentration ratio as expected. At ratio of 0.02 (mg/mg), τ =1.7 h. At lower mass ratios of 0.015 (mg/mg) and 0.005 (mg/mg) the time constant increases to 2.2 and 2.6 h, respectively, indicating that at higher concentrations Au DADs induce liposome leakage more rapidly. The characteristic times for Au TAN and Au PVP at a high mass concentration ratio of 0.02 (mg/mg) was found to be 2.6 and 3.6 h respectively, showing their slow interaction with lipid bilayers compared to positively charged Au DADs even at high concentration ratio (*i.e.* 0.02). K_L describes how fast ENMs interact with the lipid bilayer, depends on the surface functionality, and may also depend on the particle size.

3.4. Role of freely dispersed functional compounds

We also examine the effect of the surface functionalization compounds on the liposomes directly to ensure that the functionalized particle is disrupting the liposome rather than surface functional groups that may be freely dispersed in the solution, To do this, we compare the leakage induced by Au DAD with its filtrate (potentially containing free DADMAC) and free DADMAC solution freshly prepared. The filtrate was obtained by passing the original high concentrated Au DADs stock solution (1500 ppm) through a 3kDa ultrafiltration filter. We then diluted the filtrate to the concentration we used in our experiments. Figure 2 compares the induced leakage after 6 hours, L_∞, by Au DADs at 60 ppb, prepared DADMAC solution at 700 ppb (equivalent to that mass of DADMAC present on Au DAD surface estimated by gold to DADMAC mass ratio of 1 to 11.5 reported by the supplier), Au DAD filtrate potentially containing DADMAC, and the control solution (*i.e.*, buffer electrolyte). We observe insignificant leakage by DADMAC solution, filtrate, or control relative to the Au DADs. The finding indicates that the functional group DADMAC does not induce leakage on its own and has to associate with ENMs to cause lipid bilayer

leakage. The result is consistent with previous work that indicates that cationic lysozymes do not exert permeabilizing effect on liposomes unless associated with a tubular nanostructure (*i.e.*, CNTs).[43]

3.5. Impact of particle dosage on liposome leakage

We measured the steady state liposome leakage due to Au DAD and melittin over a wide range of concentration ratios from 0.001 to 0.02 (mg/mg) (corresponds to Au DAD concentration of 6 to 185 ppb) as reported in Figure 3A. The upper axis of Figure 3A shows Au DAD and melittin by mass concentration and the lower x-axis shows mass of ENMs per lipid mass. Melittin induces complete liposome leakage at a mass ratio ≥ 0.01 (mg/mg), which is similar to Au DADs. However, melittin is more effective in inducing leakage at a lower mass ratio, especially in the range of 0.0025 to 0.005 (mg/mg). For example, at mass ratio of 0.005 (mg/mg), melittin causes ~75% leakage where Au DADs only cause 40%. Both Au DAD and melittin induced leakage increases with concentration that follows a sigmoidal shape. This sigmoidal behavior is common to wide variety of chemical systems including disassociation, titration, as well as dose response curve in toxicity studies.[61,62] We calculated the mass effective concentration (EC50) of melittin and Au DAD required to reach 50% leakage as 18 and 32 ppb (mass concentration ratio of 0.003 and 0.0064 (mg/mg), respectively. These EC50 values are determined using the trimmed Spearman-Karber (TSK) dose response model, a statistical method which calculates the values by fitting the data to a sigmoidal dose response curve.[63]

Our melittin concentration dependency curve reported here follows the same trend as the previous study (Benachir *et. al*, 1995) in which similar PC lipid vesicles were used. Goodman *et al.* also showed that leakage of negatively charged SOPC/SOPS vesicles increased with increasing mass concentration of 2 nm Au DADs, although they never reported a complete liposome leakage at steady state.[44] In Goodman's study, the Au concentration ranges from 0.4 to 1.72×10^2 ppb which resulted in 12 and 50% leakage, respectively. Potential reasons for this discrepancy can be related to the lower number density of their system and multilamellar liposome structure they used. It is known that liposomes with a size larger than 200 nm have a multilamellar structure,[45] which are more resistant against permeabilization than unilamellar ones.[47] Alternatively, the nanomateral size can play a role on the mechanism by which they induce leakage, it has been shown that 2 nm amine coated Au ENMs with positive surface charge disrupt supported lipid bilayer by aggregating on the surface and expanding the pre-existing defects while positively charged 50 nm amine coated Si ENMs are capable of directly inducing defects (creation of pores) on the bilayer.[22] It is also likely that the number of Au DADs in the Goodman[44] study was not high enough to induce 100% leakage for a given amount of liposomes, but number density ratio (ENM to liposomes) cannot be calculated since they did not report the lipid concentration.

We also plot the steady state leakage results of Au DAD and melittin as a function of the ENM number density as shown in Figure 3B. The top x-axis shows the absolute number density per mililiter, while the bottom axis shows the calculated number of ENMs/melittin (n_P) normalized by the number of liposomes n_{LP}. We calculate Au ENMs number density as,

$$n_P = \frac{c_p N_A}{\left(\frac{2}{3}\right)\pi\left(\frac{d_P}{a}\right)^3} \quad (4)$$

where C_P is the molar concentration of Au ENMs, N_A is the Avogadro number, d_P is the measured ENM mean diameter, and a is the number of atoms per unit cubic cell, 4 for gold with a cell length of 4.0786 Å.[64] We estimated the number of melittin macromolecules per milliliter by multiplying melittin molar concentration by the Avogadro's number. We estimate the number of liposomes per milliliter by two methods, using either lipid head group surface area or molecular volume of DOPC lipids, as presented in the supporting information (SI). The two methods yield a similar number density of liposomes at 3.7×10^{10} mL^{-1}. Our number density ratio result for melittin is close to the value (*i.e.*, 250) reported by Benachir *et al.*[40] They estimated this value by using a statistical model for their system consisting of melittin and 100 nm POPC vesicles. The small difference between the two values may be attributed to the different calculation methods and lower resistivity of POPC liposomes against disruption they used compare to our DOPC liposomes.[49]

In contrast to the mass results, Figure 3B shows that Au DADs are more effective than melittin, per ENM, in inducing liposome leakage. For example, it requires roughly 350 melittin macromolecules per liposome compared to only one Au DAD particle to cause complete leakage. This suggests that in contrast to melittin, one Au DAD particle can induce a defect on a liposome resulting in complete release of dye. It can also be inferred that Au DAD-induced release of CF follows all-or-none pathway leading to two different vesicle populations: the intact vesicles with trapped dye at its initial concentration and the empty vesicles having released entirely their CF content. This leakage data is supported by TEM images obtained from liposome and ENM solutions as shown in Figure 4. The TEM micrograph shows that only one particle is associated with each liposome. This small number, *i.e.* one particle per liposomes, suggests that the leakage is more likely due to the formation of well-defined pores by particles rather than to collective membrane perturbation. A single Au DAD can perturb the lipid bilayer affecting its impermeability integrity. It is not clear from these images if the nanoparticles sit on the bilayer surface or are inside the liposomes.

3.6. Mechanism of lipid bilayer disruption by ENMs

Determining the physical disruption mechanism by which the Au DADs mediate liposome leakage is important to gain insight into how ENM may interact with cell membranes and exert toxicity. Recently, it has been shown by Leroueil *et. al* that positively charged nanoparticles generate holes on lipid bilayers supported on silica surfaces.[22] They show that 2 nm Au nanoparticles interact with lipid bilayer by aggregating on lipid bilayer surface diffusing to the existing defects and expanding them, while larger silica nanoparticles (50 nm) with same surface functionality are capable of formation of holes following addition to lipid bilayer. Prior studies have also indicated that polymeric ENMs with a diameter between 8 to 10 nm cause formation and growth of holes in model membranes whereas this ability is reduced by particles smaller than 6 nm.[21] Our number density ratio based data, shown in figure 3, and the supportive TEM images, suggest one 10 nm Au DAD particle is sufficient to disrupt the bilayer and release the entire encapsulated marker. We hypothesize that the disruption results from the creation of pores on the lipid bilayer, or extracting lipids from the bilayer (*i.e.* wrapping the bilayer molecules around them), leading to the release of encapsulated dye.

Some studies suggest that at higher concentrations of ENMs and melittin are capable of disrupting the lipid bilayer by inducing aggregation of liposomes thus changing their morphology or size.[57,65] Chen *et al.* examined interaction of anionic superparamagnetic iron oxide (SPIO) particles and lipid bilayers by adding them to a suspension of cationic liposomes. They have shown that particles drive vesicles to fuse together resulting in significant increase in their size which at higher particle concentrations results in bilayer deformation and flattening.[65] The lowest ENM to lipid mass ratio they used is more than

two orders of magnitude greater than what we have used here. To test the liposome fusion hypothesis in our system, we measured the hydrodynamic size change of liposomes before and after adding melittin and Au DADs at the m_P/m_{LP} mass ratio of 0.01 (mg/mg), at which 100% leakage occurs, as shown in Figure 3A. The result (not shown) indicates that melittin causes the liposome size to increase by 50%, while liposome size in the control sample without melittin remains unchanged. Melittin induces leakage by creating pores on the lipid bilayer,[35,49] it has also been shown that in the presence of melittin liposomes fuse together into larger liposomes while maintaining their structure even after complete leakage of their encapsulated marker.[66] In contrast, we only observed minimal increase in liposome size in the presence of Au DADs after 6 h (*i.e.* the point of complete leakage) compared to melittin. These results, in combination with the TEM images, suggest that fusion and morphological changes of liposomes are not the dominant phenomenon in inducing leakage at low ENM to lipid ratios, e.g. Au DAD in this study.

3.7. Effect of surface functionality of ENMs on lipid bilayer leakage

Figure 5 reports the leakage induced by 10 nm TiO2 and Au ENMs with several different surface functionalities. In these experiments, we add 60 ppb of ENMs to 6 ppm of liposomes at mass concentration ratios of 0.01 (mg/mg) and report the leakage at steady state (*i.e.* after 6 h). We see that the measured liposome leakage is a strong function of surface charge. Au DAD and TiO_2 DAD induce strong induce leakage (>80%) while only marginal leakage is measured for negatively charged Au TAN, Au PVP and TiO_2 SOD. We attribute the low leakage induced by negatively charged ENMs to electrostatic repulsion by negatively charged liposomes. A prior study showed that single walled carbon nanotubes (SWNTs) coated with positively charged proteins caused the leakage of negatively charged liposomes, while uncoated SWNTs had a minimal effect.[43] Their results also showed minimal leakage induced by negatively charged ENMs in a good agreement with our observations. Our previous work on adsorption of ENMs to lipid bilayers also suggest that the electrostatic interactions are largely control nonspecific binding of ENMs to a bilayer surface.[23,24] Collectively, there is strong evidence that surface functionality, which determines the ENM surface charge, plays a key role in the interaction of metallic and metal oxide ENMs with DOPC lipid bilayer vesicles, and changing the core composition have an insignificant effect.

4. SUMMARY

In this paper, we use fluorescence spectroscopy to detect leakage from unilamellar liposomes upon their exposure to 10 nm ENMs with different surface functionalities and core compositions. We detected leakage at ENM concentrations down to 30 ppb (corresponding to mass concentration ratio of 0.005 (mg/ml)). We found that liposome leakage is time dependent and increases with ENM number density. Our data suggests that leakage is mediated by electrostatic interactions which are primarily governed by the ENM surface functional groups and not dependent on the particle core composition. Our results demonstrate that a single Au DAD can induce complete leakage from a liposome suggesting an all-or-none mechanism. It is not clear if the leakage is caused by particles passing through the membrane, the formation of pores on the membranes, or particles extracting lipid molecules.

Given that cellular membrane disruption is one of the potential mechanisms leading to nano-toxicity, probing the lipid bilayer disruption may prove a promising alternative to cell studies to preliminarily screen the cytotoxicity for a wide range of ENMs. Liposomes are simple analogs to cell membranes and are more facile and repeatable to produce and manipulate than cells which makes them amenable to use in high-throughput assays. Additional research is needed to investigate the mechanisms by which ENMs interact with lipid bilayers and how ENM and lipid properties govern the interaction.

Supplementary Material

Refer to Web version on PubMed Central for supplementary material.

Acknowledgments

Financial support was provided by the United States Department of Energy under Award No. DE-FG02-08ER64613 with Daniel Drell as program manager, National Science Foundation grant number CBET-0932885, NIH Grand Opportunities (RC2) program through NANO-GO NIEHS grant DEFG02-08ER64613, and Semiconductor Research Corporation task number 425.025. We thank David Lowery from the Life Sciences Electron Microscopy Laboratory at ASU for assistance in obtaining TEM images of gold nanoparticles deposited on the liposomes. William Walker prepared the table of content (TOC) graphic.

References

1. Colvin VL. The Potential Environmental Impact of Engineered Nanomaterials. Nat Biotech. 2003; 21:1166–1170.
2. [accessed Mar 14: 2012] New Nanotechnology Consumer Products Inventory. http://www.wilsoncenter.org/article/new-nanotechnology-consumer-products-inventory
3. Khlebtsov N, Dykman L. Biodistribution and Toxicity of Engineered Gold Nanoparticles: a Review of in Vitro and in Vivo Studies. Chem Soc Rev. 2011; 40:1647. [PubMed: 21082078]
4. Kihara T, Zhang Y, Hu Y, Mao Q, Tang Y, Miyake J. Effect of Composition, Morphology and Size of Nanozeolite on Its in Vitro Cytotoxicity. Journal of Bioscience and Bioengineering. 2011
5. Jiang X, Ro cker C, Hafner M, Brandholt S, Do rlich RM, Nienhaus GU. Endo -and Exocytosis of Zwitterionic Quantum Dot Nanoparticles by Live HeLa Cells. ACS nano. 2010
6. Li PR, Wei JC, Chiu YF, Su HL, Peng FC, Lin JJ. Evaluation on Cytotoxicity and Genotoxicity of the Exfoliated Silicate Nanoclay. ACS Appl Mater Interfaces. 2010; 2:1608–1613. [PubMed: 20568705]
7. Perreault F, Bogdan N, Morin M, Claverie J, Popovic R. Interaction of Gold Nanoglycodendrimers with Algal Cells (Chlamydomonas Reinhardtii) and Their Effect on Physiological Processes. Nanotoxicology. 2011:1–12.
8. Hossain S, Chowdhury EH, Akaike T. Nanoparticles and Toxicity in Therapeutic Delivery: The Ongoing Debate. Therapeutic Delivery. 2011; 2:125–132. [PubMed: 22833937]
9. Lee K, Lee H, Lee KW, Park TG. Optical Imaging of Intracellular Reactive Oxygen Species for the Assessment of the Cytotoxicity of Nanoparticles. Biomaterials. 2011
10. Park J, Lim DH, Lim HJ, Kwon T, Choi J, Jeong S, Choi IH, Cheon J. Size Dependent Macrophage Responses and Toxicological Effects of Ag Nanoparticles. Chem Commun. 2011; 47:4382.
11. Bottrill M, Green M. Some Aspects of Quantum Dot Toxicity. Chem Commun. 2011
12. Thakor AS, Luong R, Paulmurugan R, Lin FI, Kempen P, Zavaleta C, Chu P, Massoud TF, Sinclair R, Gambhir SS. The Fate and Toxicity of Raman-Active Silica-Gold Nanoparticles in Mice. Science Translational Medicine. 2011; 3:79ra33.
13. Harper SL, Carriere JL, Miller JM, Hutchison JE, Maddux BLS, Tanguay RL. Systematic Evaluation of Nanomaterial Toxicity: Utility of Standardized Materials and Rapid Assays. ACS Nano. 2011; 5:4688–4697. [PubMed: 21609003]
14. Ye, J.; Shan; Liu, AL. Chapter 6 Functionalization of Carbon Nanotubes and Nanoparticles with Lipid. Vol. 8. Academic Press; 2008. p. 201-224.
15. Nel AE, Mädler L, Velegol D, Xia T, Hoek EMV, Somasundaran P, Klaessig F, Castranova V, Thompson M. Understanding Biophysicochemical Interactions at the Nano bio Interface. Nat Mater. 2009; 8:543–557. [PubMed: 19525947]
16. Mueller P, Rudin DO, Tien HT, Wescott WC. Reconstitution of Cell Membrane Structure in Vitro and Its Transformation into an Excitable System. Nature. 1962; 194:979–980. [PubMed: 14476933]
17. Lacerda L, Raffa S, Prato M, Bianco A, Kostarelos K. Cell-penetrating CNTs for Delivery of Therapeutics. Nano Today. 2007; 2:38–43.

18. Verma, Ayush. Francesco Stellacci Effect of Surface Properties on Nanoparticle Cell Interactions. Small. 2010; 6:12–21. [PubMed: 19844908]
19. Yu J, Patel SA, Dickson RM. In Vitro and Intracellular Production of Peptide-Encapsulated Fluorescent Silver Nanoclusters. Angewandte Chemie International Edition. 2007; 46:2028–2030.
20. Hong S, Bielinska AU, Mecke A, Keszler B, Beals JL, Shi X, Balogh L, Orr BG, Baker JR, Banaszak Holl MM. Interaction of Poly(amidoamine) Dendrimers with Supported Lipid Bilayers and Cells: Hole Formation and the Relation to Transport. Bioconjugate Chem. 2004; 15:774–782.
21. Mecke A, Majoros IJ, Patri AK, Baker JR, Banaszak Holl MM, Orr BG. Lipid Bilayer Disruption by Polycationic Polymers: The Roles of Size and Chemical Functional Group. Langmuir. 2005; 21:10348–10354. [PubMed: 16262291]
22. Leroueil PR, Berry SA, Duthie K, Han G, Rotello VM, McNerny DQ, Baker JR, Orr BG, Banaszak Holl MM. Wide Varieties of Cationic Nanoparticles Induce Defects in Supported Lipid Bilayers. Nano Lett. 2008; 8:420–424. [PubMed: 18217783]
23. Hou WC, Moghadam BY, Westerhoff P, Posner JD. Distribution of Fullerene Nanomaterials Between Water and Model Biological Membranes. Langmuir. 2011; 27:11899–11905. [PubMed: 21854052]
24. Hou WC, Moghadam BY, Corredor C, Westerhoff P, Posner JD. Distribution of Functionalized Gold Nanoparticles Between Water and Lipid Bilayers as Model Cell Membranes. Environ Sci Technol. 2012; 46:1869–1876. [PubMed: 22242832]
25. Hristovski KD, Westerhoff PK, Posner JD. Octanol-water Distribution of Engineered Nanomaterials. Journal of Environmental Science and Health, Part A. 2011; 46:636–647.
26. Ramachandran S, Kumar GL, Blick RH, Weide DW. van der Current Bursts in Lipid Bilayers Initiated by Colloidal Quantum Dots. Applied Physics Letters. 2005; 86:083901.
27. Chen J, Hessler JA, Putchakayala K, Panama BK, Khan DP, Hong S, Mullen DG, DiMaggio SC, Som A, Tew GN, et al. Cationic Nanoparticles Induce Nanoscale Disruption in Living Cell Plasma Membranes. The Journal of Physical Chemistry B. 2009; 113:11179–11185. [PubMed: 19606833]
28. Klein SA, Wilk SJ, Thornton TJ, Posner JD. Formation of nanopores in suspended lipid bilayers using quantum dots. Journal of Physics: Conference Series. 2008; 109:012022.
29. Planque MRR, de Aghdaei S, Roose T, Morgan H. Electrophysiological Characterization of Membrane Disruption by Nanoparticles. ACS Nano. 2011; 5:3599–3606. [PubMed: 21517083]
30. Paleos CM, Tsiourvas D, Sideratou Z. Preparation of Multicompartment Lipid-Based Systems Based on Vesicle Interactions. Langmuir. 2012; 28:2337–2346. [PubMed: 21988476]
31. White G, Von, Chen Y, Roder-Hanna J, Bothun GD, Kitchens CL. Structural and Thermal Analysis of Lipid Vesicles Encapsulating Hydrophobic Gold Nanoparticles. ACS Nano. 2012; 6:4678–4685. [PubMed: 22632177]
32. Vrhovnik K, Kristl J, Šentjurc M, Šmid-Korbar J. Influence of Liposome Bilayer Fluidity on the Transport of Encapsulated Substance into the Skin as Evaluated by EPR. Pharmaceutical Research. 1998; 15:525–530. [PubMed: 9587946]
33. Chatterjee S, Banerjee DK. Preparation, Isolation, and Characterization of Liposomes Containing Natural and Synthetic Lipids. Methods in Molecular Biology. 2002; 199:3–16. [PubMed: 12094574]
34. Gervais C, Dô F, Cantin A, Kukolj G, White PW, Gauthier A, Vaillancourt FH. Development and Validation of a High-Throughput Screening Assay for the Hepatitis C Virus P7 Viroporin. Journal of Biomolecular Screening. 2011; 16:363–369. [PubMed: 21343600]
35. Matsuzaki K, Yoneyama S, Miyajima K. Pore Formation and Translocation of Melittin. Biophysical journal. 1997; 73:831–838. [PubMed: 9251799]
36. Tosteson MT, Tosteson DC. The Sting. Melittin Forms Channels in Lipid Bilayers. Biophysical Journal. 1981; 36:109–116. [PubMed: 6269667]
37. Bechinger B. Structure and Functions of Channel-forming Peptides: Magainins, Cecropins, Melittin and Alamethicin. Journal of Membrane Biology. 1997; 156:197–211. [PubMed: 9096062]
38. Herbig ME, Assi F, Textor M, Merkle HP. The Cell Penetrating Peptides pVEC and W2-pVEC Induce Transformation of Gel Phase Domains in Phospholipid Bilayers Without Affecting Their Integrity†. Biochemistry. 2006; 45:3598–3609. [PubMed: 16533042]

39. Ralston E, Hjelmeland LM, Klausner RD, Weinstein JN, Blumenthal R. Carboxyfluorescein as a Probe for Liposome-cell Interactions Effect of Impurities, and Purification of the Dye. Biochimica et Biophysica Acta (BBA)-Biomembranes. 1981; 649:133–137.
40. Benachir T, Lafleur M. Study of Vesicle Leakage Induced by Melittin. Biochimica et Biophysica Acta (BBA)-Biomembranes. 1995; 1235:452–460.
41. Rex S, Schwarz G. Quantitative Studies on the Melittin-induced Leakage Mechanism of Lipid Vesicles. Biochemistry. 1998; 37:2336–2345. [PubMed: 9485380]
42. Chen Y, Bose A, Bothun GD. Controlled Release from Bilayer-Decorated Magnetoliposomes via Electromagnetic Heating. ACS nano. :85–98.
43. Hirano A, Uda K, Maeda Y, Akasaka T, Shiraki K. One-Dimensional Protein-Based Nanoparticles Induce Lipid Bilayer Disruption: Carbon Nanotube Conjugates and Amyloid Fibrils. Langmuir. 2010; 26:17256–17259. [PubMed: 20964299]
44. Goodman CM, McCusker CD, Yilmaz T, Rotello VM. Toxicity of Gold Nanoparticles Functionalized with Cationic and Anionic Side Chains. Bioconjugate Chem. 2004; 15:897–900.
45. Mayer LD, Hope MJ, Cullis PR. Vesicles of Variable Sizes Produced by a Rapid Extrusion Procedure. Biochimica et Biophysica Acta (BBA)-Biomembranes. 1986; 858:161–168.
46. Hope MJ, Bally MB, Mayer LD, Janoff AS, Cullis PR. Generation of Multilamellar and Unilamellar Phospholipid Vesicles. Chemistry and Physics of Lipids. Jun.40:89–107.
47. Sila M, Au S, Weiner N. Effects of Triton X-100 Concentration and Incubation Temperature on Carboxyfluorescein Release from Multilamellar Liposomes. Biochimica et Biophysica Acta (BBA) - Biomembranes. 1986; 859:165–170.
48. MacDonald RC, MacDonald RI, Menco BPM, Takeshita K, Subbarao NK, Hu L. Small-volume Extrusion Apparatus for Preparation of Large, Unilamellar Vesicles. Biochimica et Biophysica Acta (BBA) - Biomembranes. 1991; 1061:297–303.
49. Rex S. Pore Formation Induced by the Peptide Melittin in Different Lipid Vesicle Membranes. Biophysical chemistry. 1996; 58:75–85. [PubMed: 8679920]
50. Mueller NC, Nowack B. Exposure Modeling of Engineered Nanoparticles in the Environment. Environ Sci Technol. 2008; 42:4447–4453. [PubMed: 18605569]
51. BALLY, MB.; HOPE, MJ.; MAYER, LD.; MADDEN, TD.; CULLIS, PR. Liposomes as drug carriers: Recent trends and progress. Wiley; 1988. Novel Procedures for Generating and Loading Liposomal Systems; p. 841-853.
52. Hope MJ, Bally MB, Webb G, Cullis PR. Production of Large Unilamellar Vesicles by a Rapid Extrusion Procedure. Characterization of Size Distribution, Trapped Volume and Ability to Maintain a Membrane Potential. Biochimica et Biophysica Acta (BBA) - Biomembranes. 1985; 812:55–65.
53. Petitou M, Tuy F, Rosenfeld C. A Simplified Procedure for Organic Phosphorus Determination from Phospholipids. Analytical Biochemistry. 1978; 91:350–353. [PubMed: 9762117]
54. Théry C, Amigorena S, Raposo G, Clayton A. Isolation and Characterization of Exosomes from Cell Culture Supernatants and Biological Fluids. Current Protocols in Cell Biology. 2006
55. Zhang L, Granick S. How to Stabilize Phospholipid Liposomes (Using Nanoparticles). Nano Lett. 2006; 6:694–698. [PubMed: 16608266]
56. Lakowicz JR, Gryczynski I, Kusba J, Wiczk WM, Szmacinski H, Johnson ML. Site-to-site Diffusion in Proteins as Observed by Energy Transfer and Frequency-domain Fluorometry. Proceedings of SPIE. 1992; 1640:196–211.
57. Wessman P, Stromstedt A, Malmsten M, Edwards K. Melittin-Lipid Bilayer Interactions and the Role of Cholesterol☆. Biophysical Journal. 2008; 95:4324–4336. [PubMed: 18658211]
58. Lagergren S. Zur Theorie Der Sogenannten Adsorption Geloster Stoffe. Kungliga Svenska Vetenskapsakademiens. Handlingar. 1898; 24:1–39.
59. Ho Y, McKay G. Pseudo-second Order Model for Sorption Processes. Process Biochemistry. 1999; 34:451–465.
60. Yuh-Shan H. Citation Review of Lagergren Kinetic Rate Equation on Adsorption Reactions. Scientometrics. 2004; 59:171–177.

61. Wheat PM, Posner JD. Quantifying Mixing Using Equilibrium Reactions. Phys Fluids. 2009; 21:037101.

62. Altshuler B. Modeling of Dose-response Relationships. Environmental health perspectives. 1981; 42:23. [PubMed: 7333256]

63. Hamilton MA, Russo RC, Thurston RV. Trimmed Spearman-Karber Method for Estimating Median Lethal Concentrations in Toxicity Bioassays. Environmental Science & Technology. 1977; 11:714–719.

64. Maeland A, Flanagan TB. Lattice Spacings of Gold palladium Alloys. Can J Phys. 1964; 42:2364–2366.

65. Chen Y, Bothun GD. Cationic Gel-Phase Liposomes with “Decorated” Anionic SPIO Nanoparticles: Morphology, Colloidal, and Bilayer Properties. Langmuir. 2011; 27:8645–8652. [PubMed: 21649441]

66. Stromstedt AA, Wessman P, Ringstad L, Edwards K, Malmsten M. Effect of Lipid Headgroup Composition on the Interaction Between Melittin and Lipid Bilayers. Journal of colloid and interface science. 2007; 311:59–69. [PubMed: 17383670]

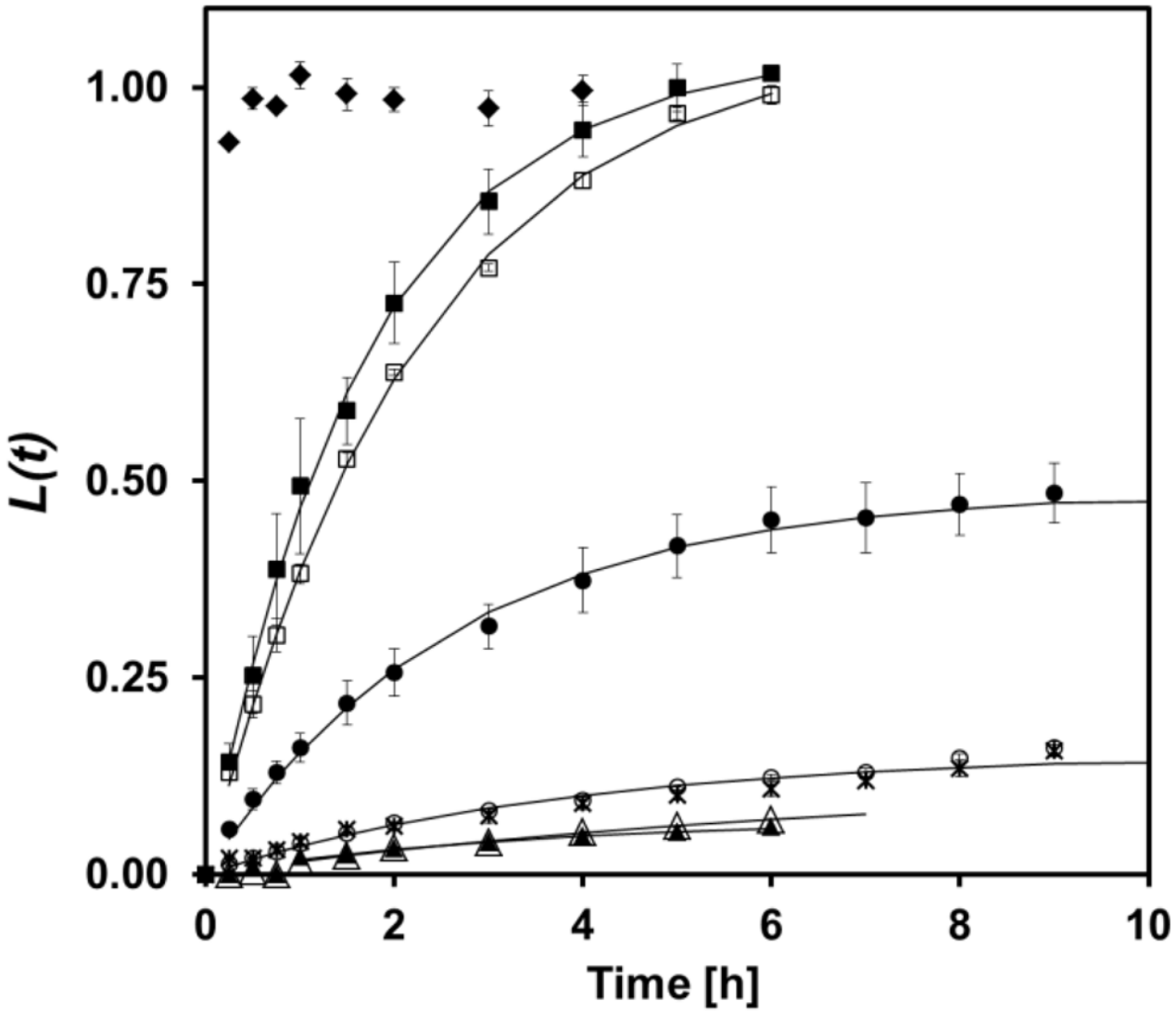

Figure 1.

Time dependency study of carboxyfluorescein (CF) dye leakage from large unilamellar liposomes (LUV) ([lipid] = 7.83 μM) induced by 10 nm gold ENMs or melittin at pH = 7.4 (20 mM HEPES), indicating the leakage in experimental samples containing melittin at a mass ratio m_P/m_{LP} = 0.005 (◆), or positively charged diallyldimethylammonium (DADMAC) coated gold ENMs (Au DADs) at ENM to lipid mass ratios of m_P/m_{LP} = 0.02 (■), 0.015 (□), 0.005 (●), or 0.002 (○), or negatively charged tannic acid coated gold ENMs (Au TAN) at m_P/m_{LP} = 0.02 (▲), or PVP coated gold (Au PVP) at m_P/m_{LP} = 0.02 (△) as well as control sample with liposomes present only (×). The error bars indicate 95% confidence interval.

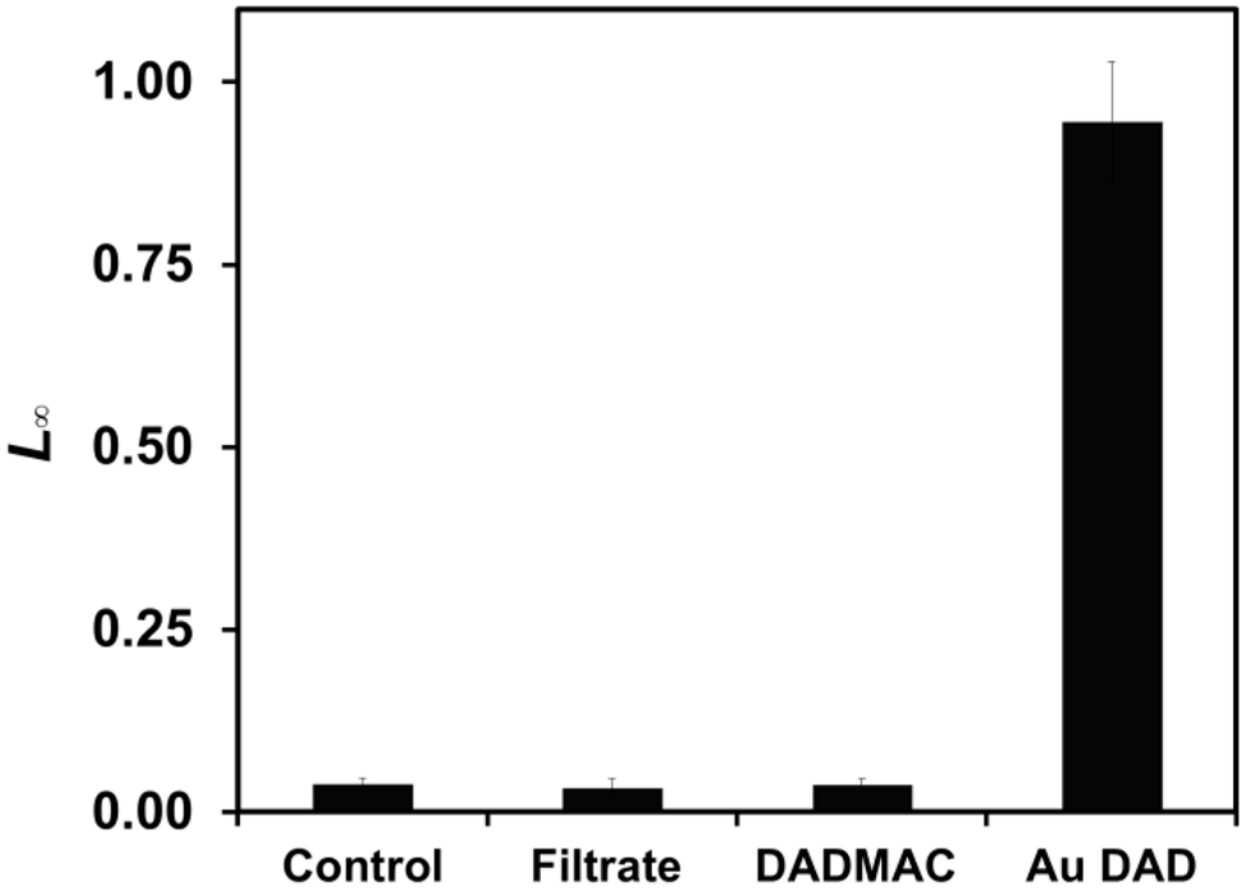

Figure 2.

Comparison of dye leakage at equilibrium from liposomes ([lipid] = 7.83 μM) induced by the positively charged DADMAC coated gold ENMs (Au DADs) (60 μg/L), poly (DADMAC), the cationic material used to coat Au DADs surface (700 μg/L), or the filtrate of Au DADs after 6 h of incubation at pH = 7.4 (20 mM HEPES). The control sample contained liposomes only. The filtrate was obtained after passing Au DADs through 3 kDa ultrafiltration membranes and was added to the samples in an equivalent amount to that in Au DADs. The error bars indicate 95% confidence interval.

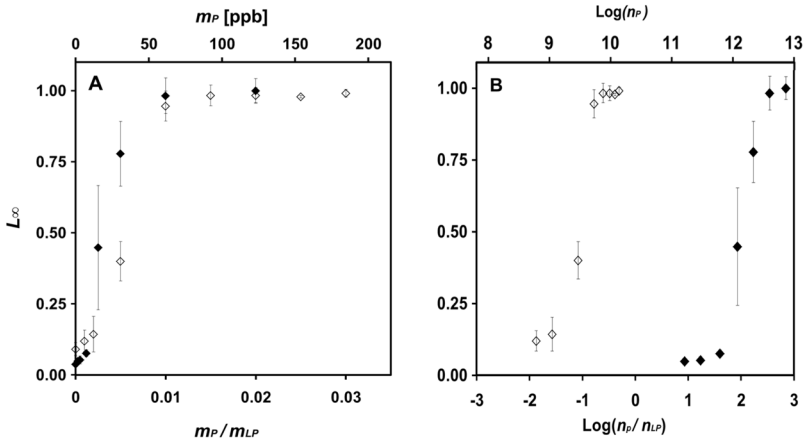

Figure 3.

Comparison of liposome leakage induced by 10 nm positively charged DADMAC coated gold ENMs (Au DADs) (◇), versus melittin (◆) as a function of (A) mass concentration(top axis), and mass ratio (lower axis), (B) number concentrations per milliliter (mL) (top axis), or number density ratio (lower axis) of Au DAD or melittin (NP) to liposome (LP) after reaching a steady state leakage at pH = 7.4 (20 mM HEPES). The error bars indicate 95% confidence interval.

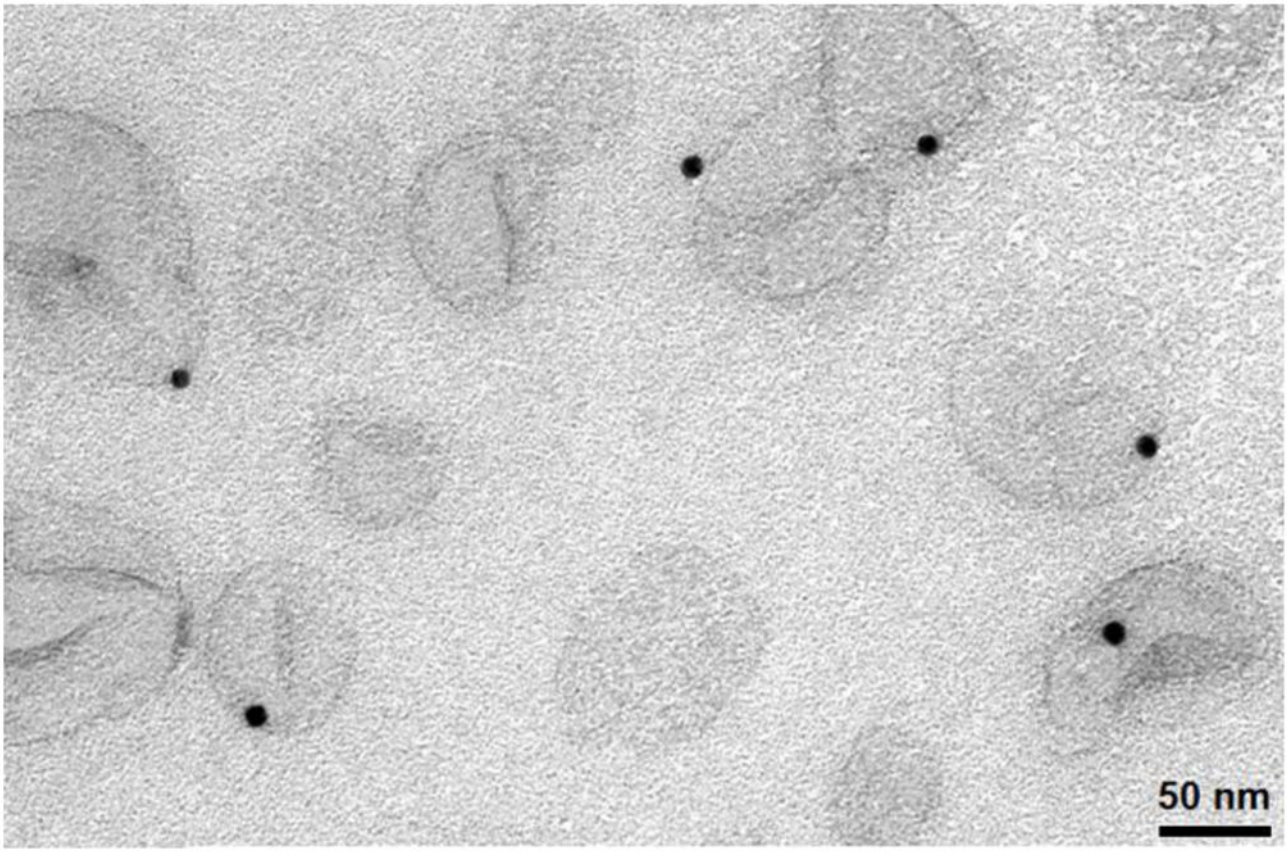

Figure 4.
TEM micrograph of liposomes and 10 nm tannic acid coated gold particles (Au TAN) that supports data in Figure 3 that only one particle per liposome is required to induce leakage.

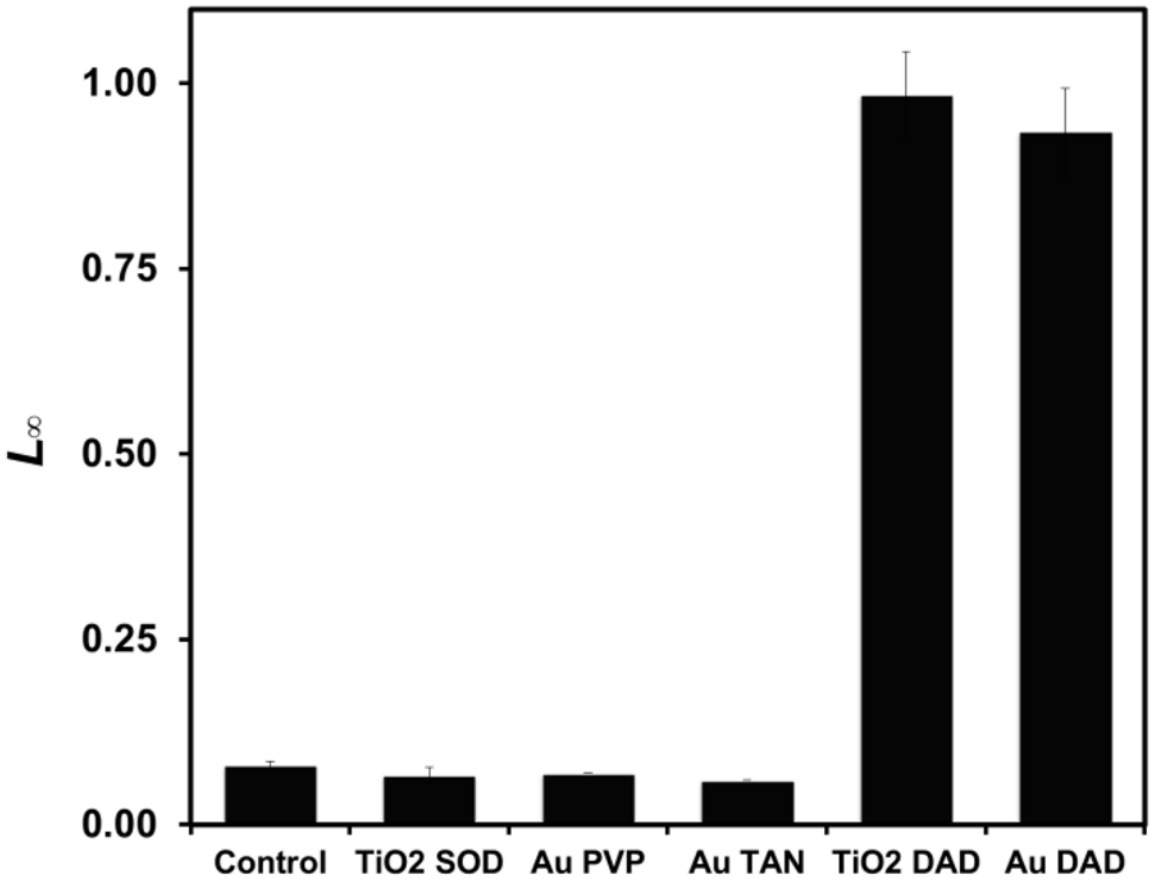

Figure 5.

Comparison of liposome leakage induced by 10 nm ENMs with different surface coatings, charge characteristics, and core compositions, indicating the percent leakage induced by positively charged DADMAC coated gold ENMs (Au DAD), negatively charged tannic acid coated gold ENMs (Au TAN), negatively charged PVP coated Au ENMs (Au PVP), positively charged DADMAC coated TiO_2 ENMs (TiO_2 DAD), as well as negatively charged TiO_2 ENMs (TiO_2 SOD), at pH = 7.4 (20 mM HEPES). The percent leakage was recorded after 6 h of interactions. The nanoparticle mass concentrations were 60 μg/L and lipid concentration was 7.83 μM. The error bars indicate 95% confidence interval.

Table 1

Kinetic parameters obtained by fitting data reported in Figure 1. Each value is reported with its corresponding 95% confidence interval.

Particle	(m_P/m_{LP})	K_L (1/h)	τ (h)
Au DAD	0.005	0.03 ± 0.0019	3.83 ± 0.52
Au DAD	0.015	0.03 ± 0.0019	2.61 ± 0.20
Au DAD	0.020	0.03 ± 0.0019	2.22 ± 0.10
Au TAN	0.020	1.11 ± 0.26	3.34 ± 0.62
Au PVP	0.020	1.90 ± 0.23	6.65 ± 0.72